Journal of Integrated
SCIENCE & TECHNOLOGY

Design and analysis of UWB patch antenna for breast cancer detection

Abhai Shankar Chaurasia,[1*] A. K. Shankhwar,[1] Rajeev Gupta[2]

[1]*Department of Electronics Engineering, Harcourt Butler Technical University, Kanpur, Uttar Pradesh, India.* [2]*Department of Electronics Engineering, Graphic Era Hill University, Dehradun, India.*

Received on: 05-Jan-2024, Accepted and Published on: 11-Jul-2024

ABSTRACT

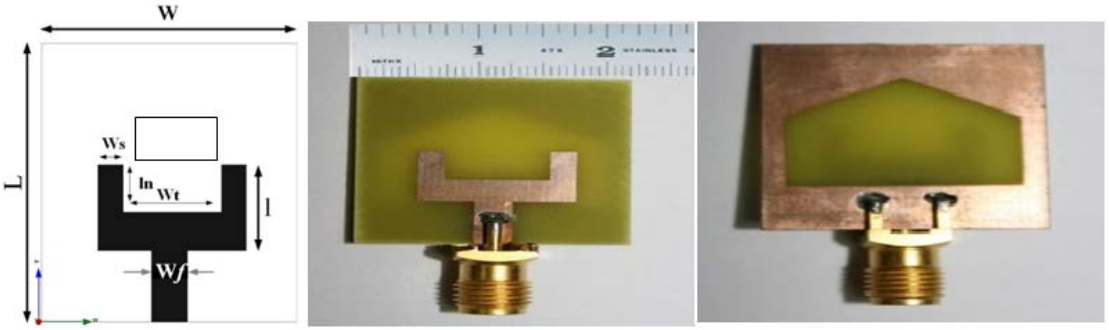

Early detection of malignant cells is inevitable, and breast cancer is a global health concern. Because of its nonionizing radiation, In recent years, microwave imaging (MWI) technology has found widespread application in the biomedical field. As a result, a low-profile UWB patch antenna for breast cancer detection technologies has been suggested in this study. With a broad operational bandwidth of 12 GHz (3.50–11.7 GHz), this antenna can operate at a low return loss of 50.83 dB at 8 GHz. To assess the performance of the antenna, The suggested antenna has been modeled with two distinct modeling programs, such as CST MWS and HFSS. The antenna can reach a maximum gain of 8.84 dBi and radiates in a quasi-omnidirectional pattern. Tumor-imitating tissue and non-tumor-mimicking tissue have been used in the building of a three-layered human body that mimics a breast phantom with varying dielectric properties. The presence of a tumor inside the breast phantom can be determined by comparing the dielectric characteristics of the tumor and the various layers of the phantom in the presence of an external radiation field. To detect malignancies with a minimum radius of 2 mm, the eight elements that make up the recommended antenna are positioned around the breast phantom. The seven-antenna array arrangement is used to evaluate the breast phantom's signal backscattering and track any notable changes in signal between the phantom's tumor cell and non-tumor state. The images produced by the backscattering signal analysis are displayed.

Keywords: Wideband, partial ground, micro-strip, Breast imaging, breast cancer, microwave imaging.

INTRODUCTION

The abnormal development of breast cells is the ultimate cause of breast cancer. According to 2020 Global Cancer Statistics, instances of breast cancer in women (i.e., 2.6 x 10^6) are more often observed than cases of lung cancer (i.e., 2.2 x 10^6).[1] Consequently, the creation of a treatment plan depends on the early discovery of breast cancer. Clinical breast examination and self-examination of the breasts, in which a medical expert physically examines the chest, are the two methods of performing breast screening.[2] Examine your breasts in front of a mirror, looking for any noticeable changes[3]: alterations in the size and form, nipple inversion, retraction, dimpling or puckering of the breast skin, hemorrhage or discharge, skin redness or soreness, unusual swelling of one upper arm, etc. Conventional breast screening techniques for clinical breast evaluation include computed tomography with nuclear magnetic resonance imaging (NMRI), positron emission tomography (PET), ultrasonography, and mammography. The diagnostic accuracy of mammography is 89.3%,[4] with a 97% high sensitivity,[4] a 64.5% specificity,[4] an 89% positive predictive value,[4] a negative predictive value of 90.9%,[4] and a limited dynamic range. However, this technique has several drawbacks, including the use of ionizing radiations,[2] the impact of breast density on sensitivity and specificity,[2] pictures with low contrast and graininess as a result of tissue sensitivity declines,[4] etc. Although ultrasound offers an 80% sensitivity and an 88.4% specificity for detecting bone structures,[5] it is not an appropriate technology for this type of imaging. Low-resolution images are produced by ultrasound, and an expert operator is needed for the

*Corresponding Author: Abhai Shankar Chaurasia, Department of Electronics Engineering, HBTU, Kanpur-UP-India.
Email: abhaihbti2009@gmail.com

Cite as: *J. Integr. Sci. Technol., 2024, 12(6), 837.*
DOI: 10.62110/sciencein.jist.2024.v12.837

inspection.[2] PET is also being considered for breast tumor screening. PET has a 68 percent sensitivity for tumors under 2 cm and 92% for those between 2 and 5 cm.[6–7] Overall, however, Its accuracy in detecting in situ carcinomas is low. (sensitivity: 2–25%). PET has a few shortcomings., such as being costly, requiring ionizing radiation,[2] having poor resolution, taking a long time to image,[2] and so on. Because of its high sensitivity (84.21%), high specificity (99.3%), and high accuracy (98.68%), CT scan is a helpful method for identifying breast cancer early. However, there are still certain drawbacks to this technique, such as the possibility of long-term consequences from repeated radiosensitive organs such as the breast being scanned with CT.[8] Another alternative to think about is the NMRI, which has a sensitivity of 94.4% and an accuracy of 72.9% when used to diagnose breast cancer in its early stages.[9] However, NMRI is not widely available and is expensive. This circumstance prompts the hunt for an additional breast imaging technique that is simple and affordable. Then microwave imaging (MWI) is a good alternative for early breast cancer screening, and the ultrawideband regime (3.1 GHz to 10.6 GHz) is the best frequency range for biomedical imaging.[10] The dielectric constant of a material can be used to quantify how much energy it can absorb from an electric field.[11] The lower the dielectric constant value, the less energy is absorbed by an electric field.[11] At the ultrawideband frequency range, there are notable differences in the dielectric characteristics of various biological tissues.[12] The quickest image inversion times are offered by MWI systems, and because the antenna serves as an antenna sensor, it is crucial to the MWI technique. In addition to transmitting the microwave signal to the intended domain, the antenna simultaneously picks up the backscattering signal.[13] Several authors looked at the ultrawideband frequency range when designing various antennas and used them to detect breast cancer early. The authors of Ref. [14] saw a tumor with a radius of 2.4 mm within the breast phantom and created a microstrip patch antenna with a dimension of 30 mm × 25 mm by considering the FR4 substrate. A modified Vivaldi antenna measuring 25 mm by 20 mm has been designed using a polyimide substrate.[15] This antenna can work in the frequency range of 3.8 GHz–4.8 GHz and 9.0 GHz–10 GHz, and it can detect tumors with a radius of 2.5 mm. A microstrip patch antenna measuring 65:4 mm x 88:99 mm was built[16] to detect breast tumors with a radius of 20 mm. To identify breast tumors early, we designed a hexagonal microstrip patch antenna on an FR4 substrate and placed eight antenna elements around the breast phantom in this paper.

RELATED WORK METHODOLOGY

Antenna Architecture. The fundamental formulas that determine the microstrip patch width (W) and patch length (PL) are as follows:[17]

$$W = \frac{C}{2 f_o \sqrt{\frac{\varepsilon_r + 1}{2}}} \quad (1)$$

We must first compute the Effective Constant Dielectric $\varepsilon_{\_eff}$ from Equation (3) and enter it into Equation (2) to get the effective length (L_eff).

$$\mathbf{L_{eff}} = \frac{\mathbf{C}}{\mathbf{2f_0\sqrt{\epsilon_{eff}}}} \quad (2)$$

Deciding on the Best Dielectric

$$\varepsilon_{eff} = \frac{\varepsilon_r + 1}{2} + \frac{\varepsilon_r - 1}{2} + (1 + 12\frac{h}{w})^{-1/2} \quad (3)$$

Step :3 As shown below, the fringing length (L) is calculated. eq.

$$\Delta L = 0.412 \frac{(\varepsilon_{eff} + 0.3)(\frac{w}{h} + 0.264)}{(\varepsilon_{eff} - 0.258)(\frac{w}{h} - 0.8)} \quad (4)$$

Step:4 Length of the path in reality (L)

$$L = L_{eff} - 2\Delta L \quad (5)$$

Calculating the Length of the Inset from eq. (6)

$$F_i = \frac{6h_s}{2} \quad (6)$$

The values of the equivalent microstrip feedline of the 50-Ohm power supply with impedance are found using Eqs. (1)–(6) (Table 1 shows the current antenna's designing parameters).

One antenna has been designed using the HFSS simulation software,[18] and the simulation has been conducted to monitor the antenna performance (return loss). This hexagonal microstrip patch antenna was first designed using an FR4 lossy material (0.02 tangent loss and 4.3 relative permittivity) as the substrate. We use five consecutive iterations to establish physically feasible results for the design of our suggested antenna (see Fig. 1). Using the values from Table 1. Figure 2 shows the final suggested antenna. We also take into consideration the CST MWS simulator[19] to construct an identical antenna and compare the two return loss curves (see Fig. 3) to validate the performance (return loss) of the single antenna that has been designed in the HFSS simulator. Fig. 3's upper panel shows the HFSS software's simulation setup. The enclosure that houses the antenna is called a radiation box, and in both simulation setups, air is taken into account inside the radiation box. In contrast, the CST MWS simulation setup is shown in the lower panel of Figure 3. It is quite difficult to construct an antenna properly for MWI. Particularly in proximity to the human body. The radiating output of an antenna may be diminished or absorbed due to the human body's role as a dielectric lossy material and the discontinuity of various dielectric properties of the human body.[20] These disadvantages must be taken into consideration while creating antennas that operate close to the human body for various applications, particularly MWI. The primary factors that led to the selection of planner patch antennas were their ease of operation, consistent emission pattern, and small, low-profile design, which made them suitable for use in microwave imaging and other UWB applications. Fig. 1 shows the antenna design geometry and configuration. A UWB antenna measuring just 21.45 × 23.45 mm2 was given in this study, and it was utilized for microwave imaging of breast tumors. When compared to the antennas described in ref [21,22,23], the antenna is smaller. The working bandwidth of the suggested antenna is 3.49 to 12 GHz. Both modeling and experimentation are used to observe the antenna's

performance. An antenna array is constructed to evaluate the performance of the recommended antenna for MWI.

Table 1. List of the recommended antenna's design parameters.

Parameters	**Dimensions (mm)**
Patch Width (w)	21.45
Patch Length (L)	23.45
Length of the Inset (Fi)	7
The patch feed line's width (w_f)	1.157
Feeding is not required for feeding (G_{pf})	1
W_t	8.22
L_n	4
Dielectric substrate (h_s)	1.6
The substrate's flexibility (ε_r)	4.6
W_s	2.11

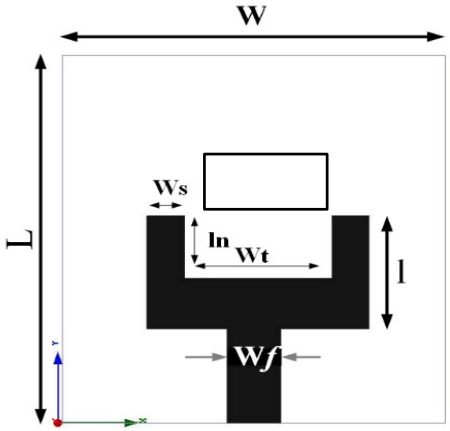

Figure 1. The antenna's geometry: upper view

When used to encircle a breast phantom in microwave imaging, the suggested antenna performs exceptionally well. As the suggested antenna is being designed, various patch shapes are tested.

RESULT OF MEASUREMENT AND SIMULATION

The proposed antenna has been simulated using the High-Frequency Structural Simulator (HFSS) and Computer Simulation Technology (CST). The suggested antenna's performance is examined after it has been fabricated. Initially, the UWB performance is observed by simulating various patch shapes of antennas. By changing the slot's dimensions and form, one can achieve decent impedance matching by strengthening the coupling between the feed line and the rectangular slot patch. Figures 2(i), 2(ii), 2(iii), and 2(iv) depict the top, bottom, and side perspectives of the fictitious antenna image, respectively. With a return loss range of ≤ 10 dB, Fig. 3 displays the return loss (S11) against frequency over the complete bandwidth from 3.49 to 12 GHz. This bandwidth is appropriate for a range of UWB uses. With a return loss range of ≤ 10 dB, Fig. 3 displays the return loss (S11) against frequency over the complete bandwidth from 3.49 to 12 GHz.

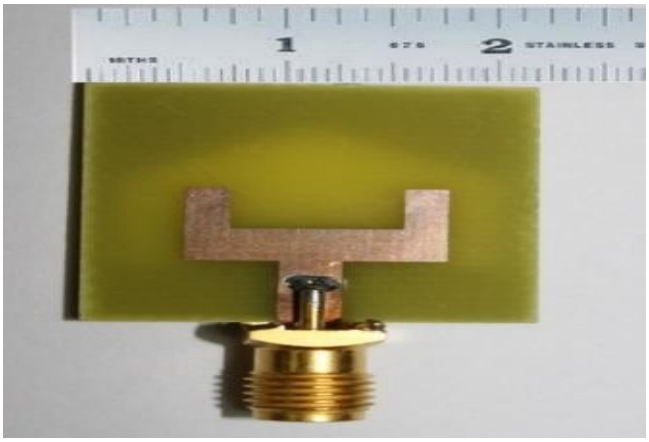

(i) ***Top view***

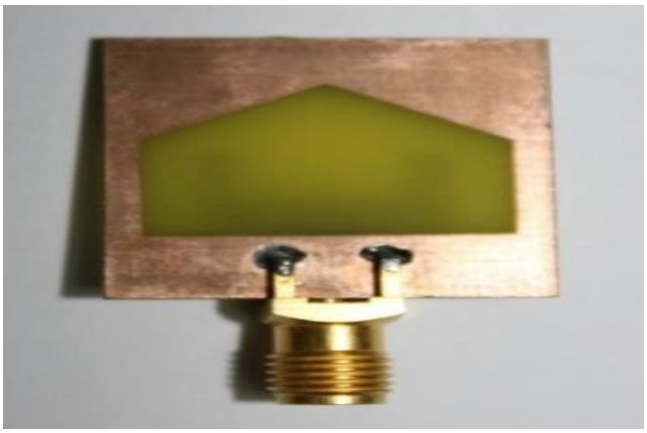

(ii) ***bottom view***

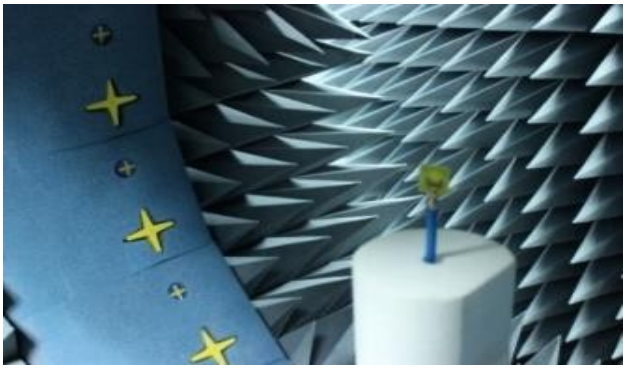

(iii)

(iv)

Figure 2. After construction, the proposed antenna picture (i) Top view; (ii) bottom view; and (iii) and (iv) measurement procedures

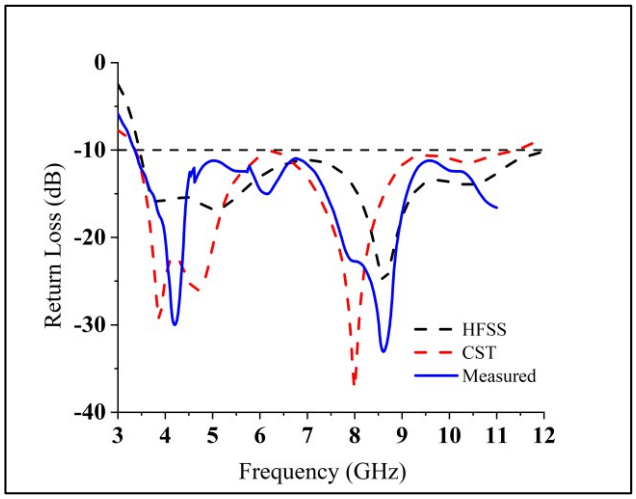

Figure 3. Return loss (S11)

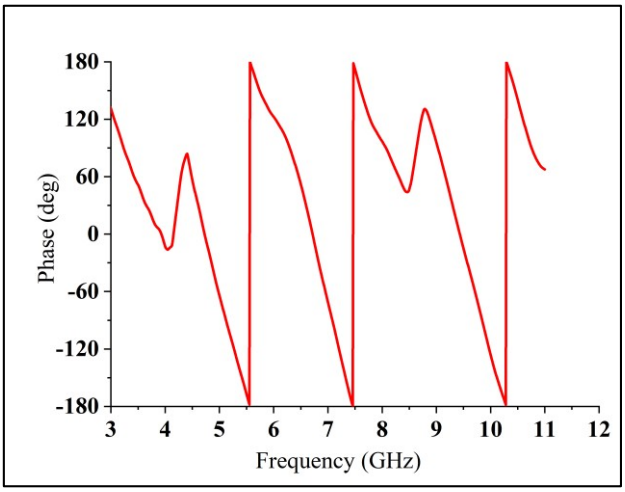

Figure 4. Phase variation of the input impedance

Figure 4 illustrates the phase deviation of the input impedance in the proposed antenna. Over the operational bandwidth, the phase variation is nearly linear. The identical delay and pulse variation are specified by the linear phase variation with respect to the operating frequency. A consistent radiation pattern is observed throughout the bandwidth.

It is evident from the preceding section that the suggested antenna performs exceptionally well in the frequency domain. However, the antenna's sound behavior in the time domain cannot be guaranteed by just having good frequency-domain properties.

Figure 5. Group delay fluctuation throughout the whole operating BW ranges from 0.96 to 1.3 ns, demonstrating acceptable phase linearity. Investigating time-domain behavior is consequently required, and this includes looking at the group delay, input-output pulse waveform, and transmission coefficient, to assess the accuracy of the suggested antenna for microwave imaging systems. The transmission coefficient |S21| is shown in Fig. 6 using two identical proposed antennas placed side by side and separated by 300 mm, taking into account far-field environments over the complete range of UWB frequencies. The measured group delay of the antenna in the side-by-side and face-to-face scenarios is defined in Fig. 7. The observation reveals two distinct changes in the group delay at 4.5 and 8.5 GHz, indicating a minor deviation from the linear phase response. Figures 8(a) and 8 (b), separately, Show the input and receiving signals side by side and face-to-face at a distance of 300 mm from the recommended antenna. Over the operational band, the transmission coefficient line in the figure has a flat magnitude. The pulse often becomes almost unidentifiable if the change is more than 50% (FF < 0.5)[20]. According to the fidelity factors of 82% and 90% for face-to-face and side-by-side orientation, respectively, there is less signal distortion while transmitting UWB impulse impulses using the recommended system. A consistent group delay indicates the strong phase linearity of the suggested antenna for the intended UWB-based microwave imaging system, a low variation transmission coefficient, and a reasonable fidelity factor.

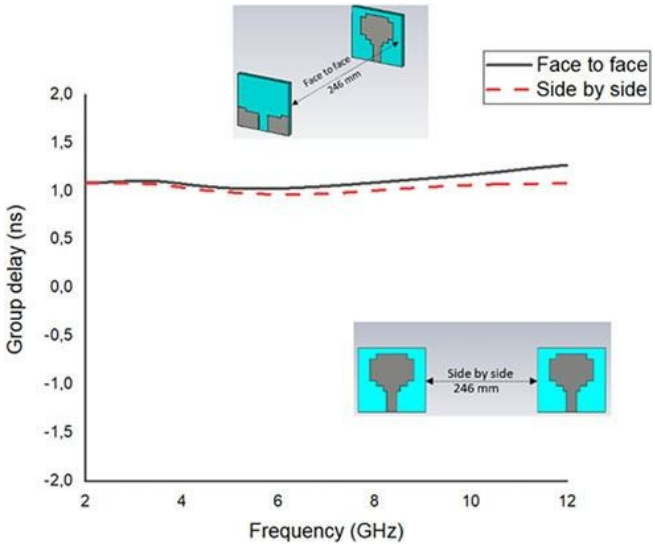

Figure 5: FtF and SbS group delay variation

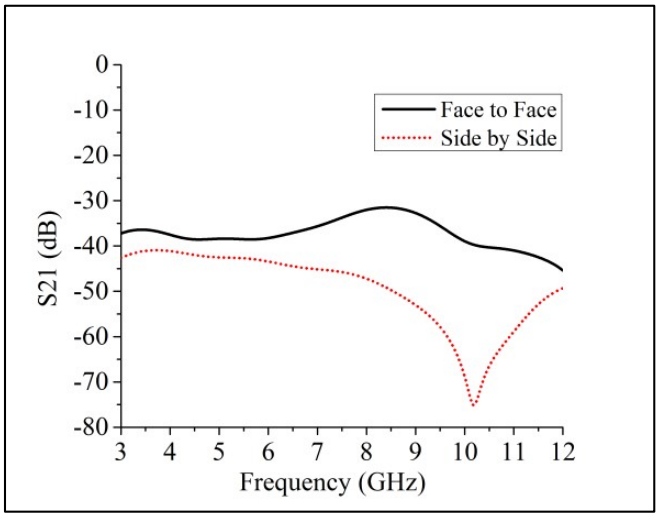

Figure 6. The transmission coefficient in both the side-by-side and face-to-face scenarios.

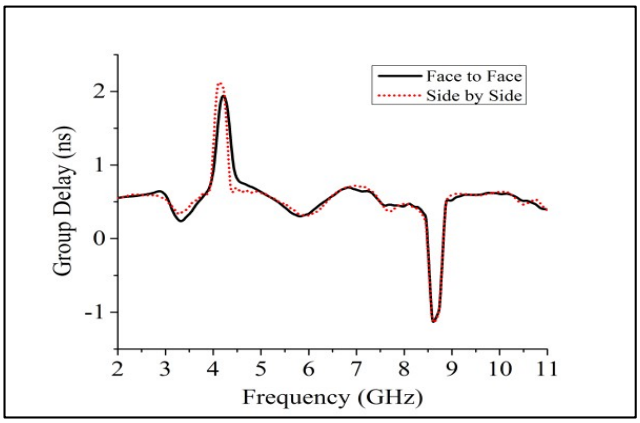

Figure 7. Group Delay in a side-by-side and in-person setting.

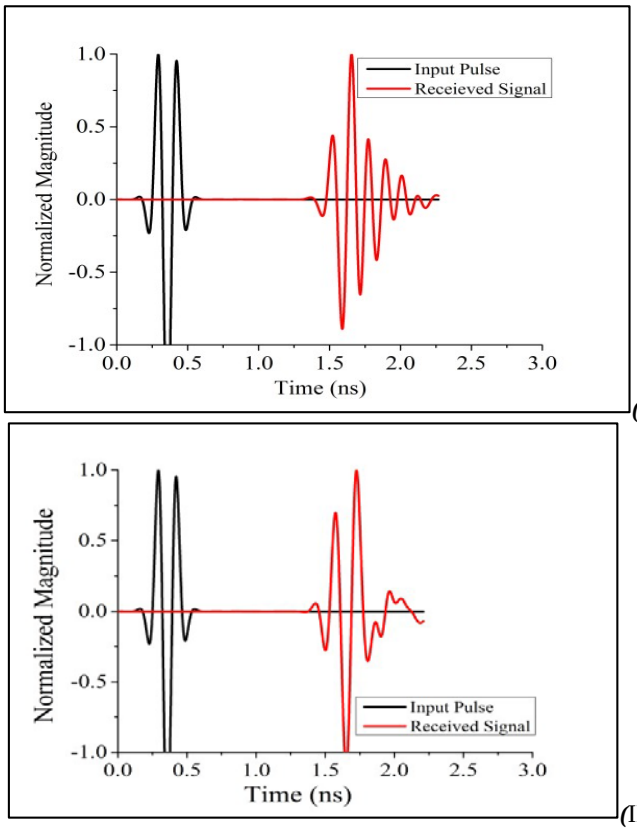

(I) (II)

Figure 8. The pulse waveforms received and input in both the (I) face-to-face and (II) side-by-side scenarios.

Fig. 9 depicts the expected antenna array system design for breast imaging. The main objective is to determine the difference in the backscattering signal with and without a high dielectric inclusion tumor present. The high dielectric constant system uses a similar phantom breast with an internal tumor. The skin and breast tissue layers make up the two layers that make up the electrical

characteristics of the breast phantom. The breast tissue layer has a conductivity of 0.132 S/m and 5.17 as the dielectric constant, measuring 8.75 cm in width. The skin layer is 2.5 mm wide, with a conductivity of 1.49 S/m, and a dielectric constant of εr=38. A tumor with a diameter of 10 mm and a dielectric constant close to 67 is situated 6 mm inside the skin layer. Because of its high water content, Generally speaking, tumor cells have a higher dielectric constant than healthy breast tissue, such as fat. To monitor the 7 antenna array system's performance, the correlation between S11, S21, S31, S41, S51, S61, and S71 is looked at. By positioning the antenna 45 mm from the surface of the breast phantom's surrounds, the S-parameters can be determined. The antennas are removed by 25 degrees, and the reflection coefficient is also recorded. The frequency range for the antenna array is 3–12 GHz.Figure. The antenna array system's s-parameters for two distinct configurations are shown in Figure 10: one with and one without a tumor cell inside the phantom. For these two cases, a notable shift in the received signal is noted. The array model's simulated imaging findings for the breast tumor detection system are displayed in Fig. 11. The two frequencies at which the backscattering signals occur are 3.5GHz and 6.5GHz. Because the tumor cell and normal breast tissue have different dielectric properties, the tumor cell transmits a greater proportion of signals than the latter.

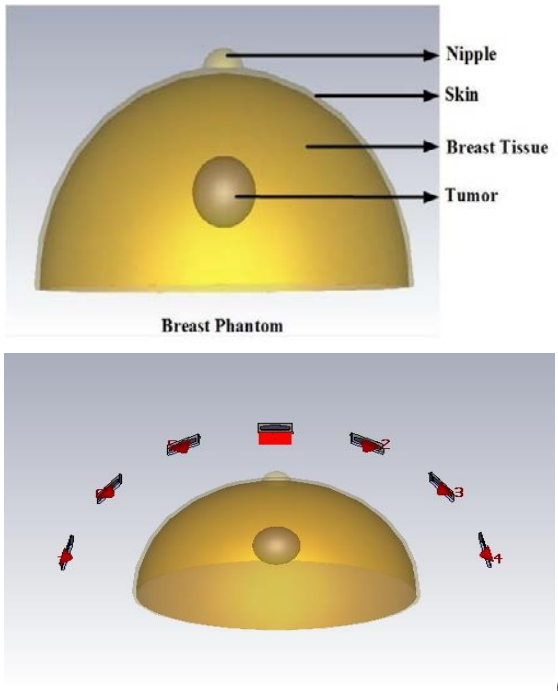

(i)

(ii)

Figure 9. Microwave imaging configuration: (i) breast phantom and (ii)antenna array arrangement encircling the phantom.

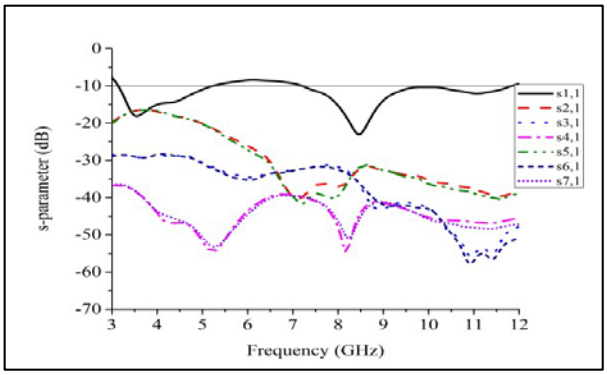

(I)

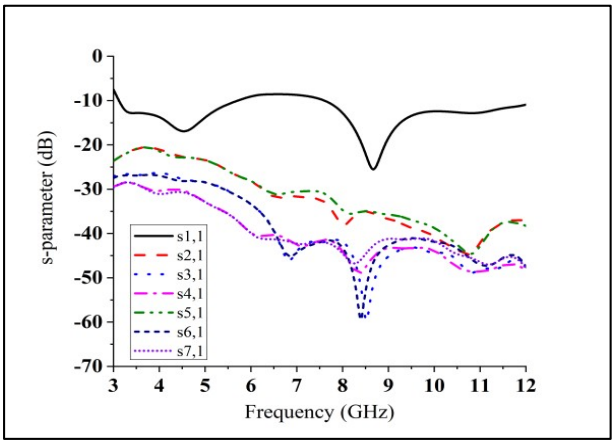

(II)

Figure 10. Antenna array S-parameters (i) with tumor and (ii) without tumor

Table 2: Analyzing the reported antenna and the suggested antenna

Antennas	BW GHz (–10 dB)	Dimension Area (mm^2)	FB (%)	Gain (dBi)	Uses
[11]	1.15–4.40	75 × 75	117.12	2.0-8.0	MWI
[17]	3.80–11.85	30 × 30	102.00	not disclosed	MWI
[21]	2.70–9.70	22.25 × 20	112.90	not disclosed	MWI
[22]	4.00–9.00	30 × 30	76.92	2.0-6.0	MWI
Suggested	3.50 - 11.7	21.45 × 23.45	109.8	6.36	MWI

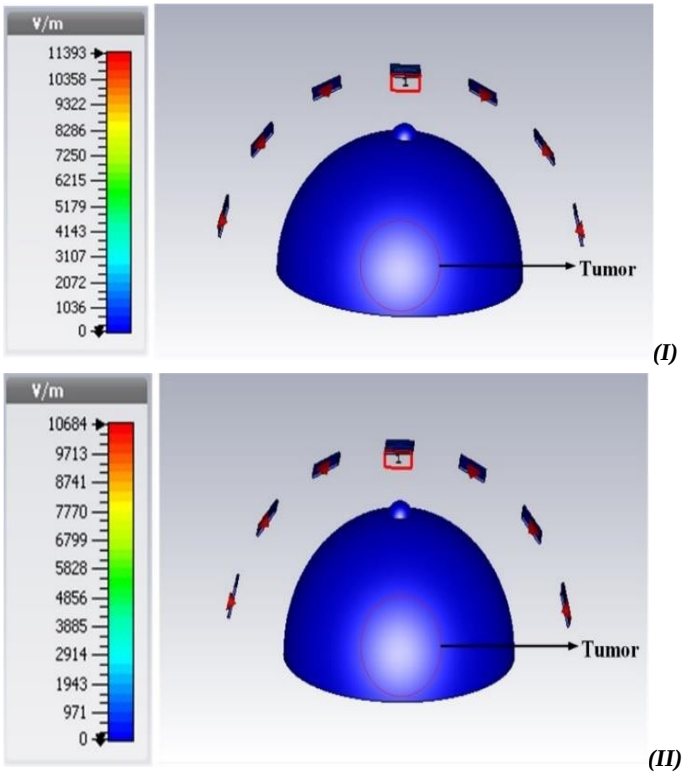

(I)

(II)

Figure 11. Antenna array microwave imaging results at (a) 3.5GHz and (b) 6.5GHz

Consequently, the percentage of signals that scatter inside the normal tissue is higher than that of the tumor cell. Therefore, the density of the received signals towards the tumor cell is great.[24]

Table 2 presents a comparison between the proposed and reported antennas. The parameters that are taken into consideration are application, antenna gain, geometry, and bandwidth. It has been noted that the suggested antenna performs better than the antennas that have been reported.[11,17,21,22]

Conclusions

This study presents the design and realization of a compact patch antenna with dimensions of 21.45 × 23.45 mm2. A breast phantom is surrounded by a seven-antenna element array that is intended for screening. Analyzing the simulated and experimental data, the performance of a single antenna for UWB characteristics was confirmed. Within the 109.8% (3.49–12 GHz) bandwidth, the suggested antenna exhibits good impedance matching, strong gain, a larger bandwidth that is highly effective, and constant omnidirectional radiation patterns. scenarios in the frequency domain as well as the time domain, the antenna performs well. The breast phantom measurement system uses the antenna array to locate breast tumors. The array technology was a perfect fit for microwave breast imaging because of the antenna-backscattering signal changing when a tumor was present inside the phantom.

Conflict of Interest Statement

The authors declare that there is no conflict of interest for publication of this work.

References

1. B.S. Chhikara, K. Parang. Global Cancer Statistics 2022: the trends projection analysis. *Chem. Biol. Lett.* **2023**, 10 (1), 451.
2. P. Jaglan, R. Dass, M. Duhan. Breast Cancer Detection Techniques: Issues and Challenges. *J. Inst. Eng. Ser. B* **2019**, 100 (4), 379–386.
3. K.D. Miller, M. Camp, K. Steligo. The breast cancer book : a trusted guide for you and your loved ones; Johns Hopkins University Press, Baltimore, MD, **2021**.
4. M. Zeeshan, B. Salam, Q.S.B. Khalid, S. Alam, R. Sayani. Diagnostic Accuracy of Digital Mammography in the Detection of Breast Cancer. *Cureus* **2018**, 10 (4), 2448.
5. R. Sood, A.F. Rositch, D. Shakoor, et al. Ultrasound for breast cancer detection globally: A systematic review and meta-analysis. *J. Glob. Oncol.* **2019**, 2019 (5), 1–17.
6. K.Y. Sang, N. Cho, K.M. Woo. The role of PET/CT for evaluating breast cancer. *Korean J. Radiol.* **2007**, 8 (5), 429–437.
7. N. Avril, C.A. Rosé, M. Schelling, et al. Breast imaging with positron emission tomography and fluorine-18 fluorodeoxyglucose: Use and limitations. *J. Clin. Oncol.* **2000**, 18 (20), 3495–3502.
8. E. Desperito, L. Schwartz, K.M. Capaccione, et al. Chest CT for Breast Cancer Diagnosis. *Life* **2022**, 12 (11), 1699.
9. C.R.B. Merritt. Diagnostic accuracy of mammography, clinical examination, US, and MR imaging in preoperative assessment of breast cancer. *Breast Dis.* **2005**, 16 (3), 245–246.
10. S.S. Ahmed, J.F. Mahdi, M.A. Kadhim. Design of Ultra-Wideband Microwave Antenna Array for Detection Breast Cancer Tumours. *IOP Conf. Ser. Mater. Sci. Eng.* **2020**, 881 (1), 12112.
11. C.A. Balanis. Antenna Theory: Analysis and Design; Wiley, Hoboken, NJ. **2016**.

12. Y. Cheng, M. Fu. Dielectric properties for non-invasive detection of normal, benign, and malignant breast tissues using microwave theories. *Thorac. Cancer* **2018**, 9 (4), 459–465.
13. D. O'Loughlin, M. Adnan Elahi, E. Porter, et al. Open-source software for microwave radar-based image reconstruction. In *IET Conference Publications*; Apr, London, UK, **2018**; Vol. 2018, pp 9–13, 408,.
14. D. Bhargava, P. Rattanadecho. Microwave imaging of breast cancer: Simulation analysis of SAR and temperature in tumors for different age and type. *Case Stud. Therm. Eng.* **2022**, 31, 10184.
15. A.M. Qashlan, R.W. Aldhaheri, K.H. Alharbi. A Modified Compact Flexible Vivaldi Antenna Array Design for Microwave Breast Cancer Detection. *Appl. Sci.* **2022**, 12 (10), 4908.
16. N. Ali, J. Ahmed. Microstrip Patch Antenna Design For Breast Cancer Detection. *Proc. - 2022 Int. Conf. Eng. MIS, ICEMIS 2022* **2022**, 195, 2905–2911,.
17. T. Tewary, S. Maity, S. Mukherjee, et al. High gain miniaturrized super-wideband microstrip patch antenna. *Int. J. Commun. Syst.* **2022**, 35 (11), 5181.
18. T. Islam, S. Roy. Low-Profile Meander Line Multiband Antenna for Wireless Body Area Network (WBAN) Applications with SAR Analysis. *Electron.* **2023**, 12 (6), 1416.
19. M.S. Islam, S.M. Kayser Azam, A.K.M. Zakir Hossain, M.I. Ibrahimy, S.M.A. Motakabber. A low-profile flexible planar monopole antenna for biomedical applications. *Eng. Sci. Technol. an Int. J.* **2022**, 35, 101112.
20. N. Wongkasem. Electromagnetic pollution alert: Microwave radiation and absorption in human organs and tissues. *Electromagn. Biol. Med.* **2021**, 40 (2), 236–253.
21. A. Afifi, A. Abdel-Rahman, A. Allam, A.A. El-Hameed. Circuits and Systems (MWSCAS. In *2016 IEEE 59th International Midwest Symposium on, 2016: IEEE*; pp 1–4.
22. R. Azim, M.T. Islam, N. Misran. Compact Tapered-Shape Slot Antenna for UWB Applications. *IEEE Antennas Wirel. Propag. Lett.* **2011**, 10 (April), 1190–1193.
23. A. Gupta, A. Kansal, P. Chawla. A survey and classification on applications of antenna in health care domain: data transmission, diagnosis and treatment. *Sādhanā* **2021**, 46 (2), 68.
24. A.S. Chaurasia, A.K. Shankhwar, A. Singh. Design and analysis of the Flexible Antenna behavior for Microwave Imaging of breast cancer. *J. Integr. Sci. Technol.* **2024**, 12 (2), 727.